Skin Research and Technology 2016; **22**: 238–246
Printed in Singapore · All rights reserved
doi: 10.1111/srt.12255

Published by John Wiley & Sons Ltd
Skin Research and Technology

Potential use of OCT-based microangiography in clinical dermatology

U. Baran[1,2,*], W. J. Choi[1,*] and R. K. Wang[1]

[1]*Department of Bioengineering, University of Washington, Seattle, WA, USA and* [2]*Department of Electrical Engineering, University of Washington, Seattle, WA, USA*

Abstract: Background: Optical coherence tomography (OCT) is a revolutionary imaging technique used commonly in ophthalmology, and on the way to become clinically viable alternative in dermatology due to its capability of acquiring histopathology level details of *in vivo* tissue, non-invasively. In this study, we demonstrate the capabilities of OCT-based microangiography in detecting high resolution, three-dimensional structural, and microvascular features of *in vivo* human skin with various conditions.
Methods: A swept-source OCT system that operates on a central wavelength of 1310 nm with an A-line rate of 100 kHz is used in this study. We apply optical microangiography (OMAG) technique to visualize the structural and microvascular changes in tissue.
Results: OMAG images provide detailed visualization of functional microvasculature of healthy human skin from cheek and forehead areas, abnormal skin conditions from face, chest and belly. Moreover, OMAG is capable of monitoring the progress of wound healing on human skin from arm, delivering unprecedented detail of microstructural and microvascular information during longitudinal wound healing process.
Conclusion: The presented results promise the clinical use of OCT angiography, aiming to treat prevalent cutaneous diseases, by detecting blood perfusion, and structural changes within human skin, *in vivo*.

Key words: optical coherence tomography – optical microangiography – nevus – acne – wound healing

Accepted for publication 29 July 2015

THE VISUAL input has been the most important information for dermatologists in clinic. Typical diagnostic steps used in clinics (1) are following: (i) recognition of patterns in the cutaneous tissue; (ii) study of the patient history; and (iii) analyses of tissue histopathology in laboratory through biopsy, if necessary. Because of its invasiveness and inconvenience, the skin biopsy is usually not desirable if not necessary. Hence, the first step of visualization of the skin is a key to a comprehensive examination and accurate diagnosis. This approach is still commonly used by visual inspection of dermatologist using a magnified glass under 'cold light', relying heavily on subjective assessment.

Recently, emerging non-invasive imaging methods such as dermoscopy (2), confocal microscopy (3), and high-resolution ultrasound imaging (4) offer a comprehensive set of tools that dermatologists can utilize for state-of-the-art patient care. Dermoscopy is the most popular imaging tool used in practice. It provides magnified images of skin up to papillary dermis (D) using high-resolution prismatic loupes and a camera. It is typically used after the application of water drop with a faceplate to increase light penetration into tissue. Unfortunately, it only provides two dimensional images. On the other hand, the higher resolution (~1 μm), three-dimensional images of skin up to ~150 μm depth can be acquired using confocal microscopy. High-resolution ultrasound imaging can penetrate deeper into the tissue, but usually cannot provide adequate resolution for accurate quantitation. However, it can be useful in detecting abnormalities in the deeper layers of the skin, which would not be possible with the previously mentioned methods. Still, an alternative non-invasive imaging technique with both high-resolu-

*Equally contributed authors.

tion and good penetration depth capabilities would be instrumental in dermatology clinics.

Optical coherence tomography (OCT) is an emerging technology that is currently popular in clinical ophthalmology. It is a real-time, non-invasive 3D imaging tool capable of producing morphological images of tissue microstructures *in vivo* with a millimeter range field of view and a micron-level resolution similar to histology (5). Its working principle is analogous to ultrasound, where echoes of sound waves are used for delineating heterogeneous tissue structures. In OCT, instead of sound, light backscattering coming from tissue features is used as the imaging contrast, which in return gives superior image resolution by sacrificing penetration depth. Due to its high resolution (up to 1 μm), reasonable imaging depth (1–3 mm), and real-time imaging capability, OCT has gained more and more attention in dermatology research. By delineating wound re-epithelialization, reformation of the dermo-epidermal junction, and dermal remodeling (6), OCT has been successfully used to study non-melanoma basal cell carcinoma (7), actinic keratosis (8), inflammatory diseases (9), to quantitate structural changes in human skin during acne development (10), and wound healing (11).

In addition to its microstructural imaging capability, OCT signal can also be utilized to provide 3D blood and lymphatic angiography down to capillary level in tissue beds *in vivo* using methods called optical microangiography (OMAG) (12), and optical lymphangiography (13), respectively. Over the past few years, OMAG technique has been intensively used to study *in vivo* microvasculature of a variety of biological tissues in preclinical and clinical settings. For example, it has been used to investigate the vascular abnormalities in a psoriasis patient (14). It has also been used to study cerebral microvasculature in mice (15, 16), to image capillary morphology in human finger (17) and human oral cavity (18), and to study microvascular response to inflammation induced by tape stripping on human skin *in vivo* (19). On the other hand, OCT-based optical lymphangiography has been utilized in assessment of wound healing phases on rodents (20) and is currently under development for *in vivo* human skin imaging.

Recently, Baran et al. (21) demonstrated the first use of a functional OCT system in detecting high resolution, three-dimensional structural and microvascular features of *in vivo* human facial skin during acne lesion initiation and scar development, and introduced vascular density change as an alternative biomarker for the assessment of human skin diseases. The promising results of this work stimulated the question about the future of OCT angiography technology in dermatology clinics. Our aim in this paper was to further explore the feasibility of functional OCT in clinical use and explain its potential and limitations. We present microvascular and structural map of healthy and abnormal human skin types *in vivo*, using OCT-based techniques. The system and methods are described in Section 2. The experimental results are shown in Section 3. Section 4 provides a discussion of the implications of our results and the potential and future challenges for OCT in clinical dermatology. Finally, Section 5 provides concluding remarks.

System and Methods

In this work, we used a 1.3 μm swept-source OCT (SS-OCT) system provided by Thorlabs (OCS1310V1; Thorlabs, Inc., New Jersey, USA) for skin tissue imaging *in vivo*, upon which OMAG scanning protocol was employed to obtain microvascular image. Figure 1 shows a schematic of the system setup. The system was illuminated by a microelectromechanical (MEMS) tunable vertical cavity surface emitting laser operating at 1310 nm and capable of sweeping the lasing wavelength at 100 kHz. The spectral bandwidth of laser output was measured ~67 nm at −3 dB (an inset in Fig. 1). A Mach–Zehnder interferometer (MZI) built in the laser module provided real-time optical clocking, from which the MZI signal was detected by a dual-balanced detector connected to an external clock input of a 12 bit 500 MS/s data acquisition (DAQ) card. The optical clocking enabled OCT fringes to be evenly sampled in wavenumbers, eliminating need of wavenumber resampling and interpolation of the detected fringe signals for OCT image reconstruction.

The main output of the laser was launched into a fiber-based interferometer, where the light is evenly split into a reference arm and a sample arm using a 50/50 fiber coupler. Retro-reflected light beams from each arm were recombined at the fiber coupler, producing an interference fringe signal, which was detected

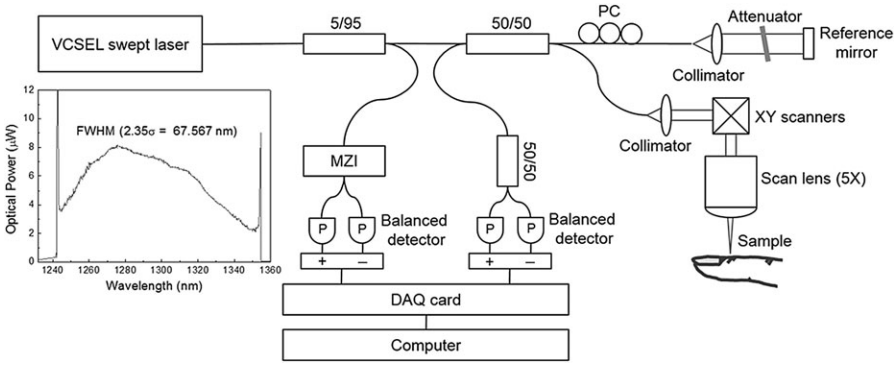

Fig. 1. A schematic of 1.3 μm swept-source OCT (SS-OCT) system for skin tissue imaging in vivo. MZI, Mach–Zehnder interferometer; P, photo-detector; DAQ card, data acquisition card; PC, polarization controller; OCT, optical coherence tomography. Inset: measured optical spectrum of laser source (18).

by the 2nd dual-balanced detector to remove the DC and autocorrelation noise in the interference signal. After linear sampling of the interference fringe signal by the DAQ card, the sampled fringe signal was converted from time domain to frequency domain using fast Fourier transform, yielding a depth dependent reflectivity profile (A-line). Acquisition of successive A-lines at different position on the sample was possible with fast transverse (*X*-axis) scanning (B-scan) of a galvo mirror, producing one OCT B-frame. With addition of slow elevational (*Y*-axis) galvo scanning (C-scan), eventually, one 3D OCT volume data could be acquired. The spatial resolution of system was experimentally measured to be 21 μm (axial) × 22 μm (lateral), and the measured sensitivity was 105 dB on average, almost constant up to depth of 4.25 mm in air (18). The optical power of incident light upon the sample was ~5.2 mW below the ANSI standards (Z136.1) for the safe use of near infrared light at 1310 nm (22).

To extract functional microvascular information from the acquired OCT data, we adopted OCT angiography as the extension of functional OCT imaging scheme, i.e. OMAG (12). OCT angiography utilizes dynamic light scattering to contrast functional blood vessel within scanned tissue volume. In general, light scattering due to moving red blood cells (RBCs) is spatiotemporally variable, unlike that due to static tissue around the vessel. This scattering property at the moving RBCs randomly changes OCT signals over time, while OCT signal at the static tissue is relatively stationary. Therefore, it is possible to extract the blood flow signal from surroundings by interrogating the variation in OCT signal, which serves as an endogenous source of contrast for blood vessel mapping. There are reported OCT angiography techniques to detect the OCT signal variation (23–26). Here, we employed the OCT angiography by the use of intensity variation, in which a blood flow image was generated by differentiating adjacent OCT intensity B frames with a time interval, but acquired at the same location (23). A repetition scanning protocol dedicated to blood flow imaging was designed and applied to OCT DAQ. In this protocol, OCT B-scans were repeated eight times at every location along the Y-direction, allowing ensemble averaging of seven blood flow images for each Y-position to increase the signal to noise ratio of blood flow signal. Numbers of A-lines in B-scan and Y-positions in C-scan could be properly set from the scanned range on tissue sample.

Subject volunteers were used in this study to demonstrate the usefulness of OMAG to delineate skin microvascular features in normal skin and skins with pathological conditions. The use of OCT/OMAG laboratory instrumentations on volunteer subjects was reviewed and approved by the Institutional Review Board of the University of Washington, and informed consent was obtained from all subjects before imaging. This pilot study followed the tenets of the Declaration of Helsinki and was conducted in compliance with the Health Insurance Portability and Accountability Act.

Results

Structural and microvasculature imaging on healthy skin

To validate functional OCT imaging of human skin tissue, we firstly imaged a nailfold. Human

nailfold is a good choice of sample for vascular imaging because of easy access and well-known vessel morphology of which disposition is in parallel to the skin surface as opposed to other tissue vascularity normal to the surface (27). In particular, we examined nailfold of fourth finger (ring finger) of left hand because of greater transparency of the skin (27). A healthy volunteer was comfortably seated at room temperature and his left hand was placed onto the sample stage under the scan lens for imaging. Figure 2 shows OCT imaging result of the nailfold of fourth finger. A representative OCT structural cross-section (Fig. 2a) delineates internal layers of proximal nailfold such as stratum corneum (SC), D, nail matrix (NM), and root of nail (RN). Corresponding blood flow image is shown in Fig. 2b in which, bright signals are attributed to blood perfusion through functional capillaries and small vessels. To visualize vessel network of the nailfold, the vasculature was reconstructed from 3D OCT angiography dataset using rendering software coded with Matlab language to create *en face* image. Figure 2d–f are *en face* images (2 mm × 2 mm) of 3D rendered vasculatures obtained from three different depth ranges (280–430 μm, 430–600 μm, 600–880 μm), representing nail bed networks in depth. At the papillary D below the SC (280–430 μm), it is observed that hair-pin looking capillary loops are regularly distributed and oblique to the skin surface (Fig. 2d) (28). At deeper D (430–600 μm and 600–880 μm), arborizing vessel plexus is visible, branching into finer secondary vessels and the capillary loops (Fig. 2e and f). Overlay of Fig. 2d and e with different colors (green, blue, and red, respectively) delineates typical vessel morphology of normal nailfold in Fig. 2c.

Moreover, facial skin tissues of another healthy volunteer were imaged with the system. In this work, we employed handheld probing scheme for easy access of light beam to the facial regions. For forehead imaging, the subject laid in supine position on a mattress with his head on a pillow and then the handheld OCT probe was gently touched on the forehead. However, the cheek imaging of the subject in seated position was conducted with contact mode of the same OCT probe. A top panel of Fig. 3 represents *en face* structure image of forehead (a), its vasculature image (b), and their overlay (c), respectively. From the overlaid image in Fig. 3c, it is noted that hair follicles are encircled by small vessels to possibly supply nutrients necessary for hair growth. Likewise, a bottom panel of Fig. 3 shows *en face* structure image of cheek (d), its vasculature image (e), and their overlay (f), respectively. Unlike in Fig 3b, vessels appear larger in

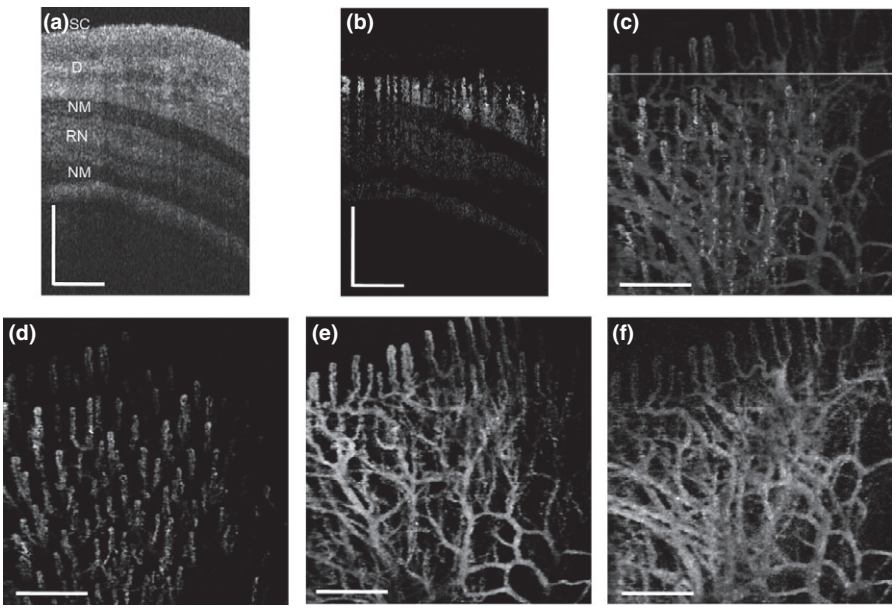

Fig. 2. In vivo OCT imaging of healthy human nailfold. (a) A representative OCT structural cross-section of nailfold of fourth finger. SC, stratum corneum; D, dermis; NM, nail matrix; RN, root of nail; OCT, optical coherence tomography. (b) A blood flow image corresponding to (a). (c) Color coded en face OCT angiography image where the horizontal line indicates the location of (a) and (b). (d–f) En face images of vasculatures obtained from different depth ranges: (d) 280–430 μm, (e) 430–600 μm, (f) 600–880 μm. Scale bars represent 0.5 mm.

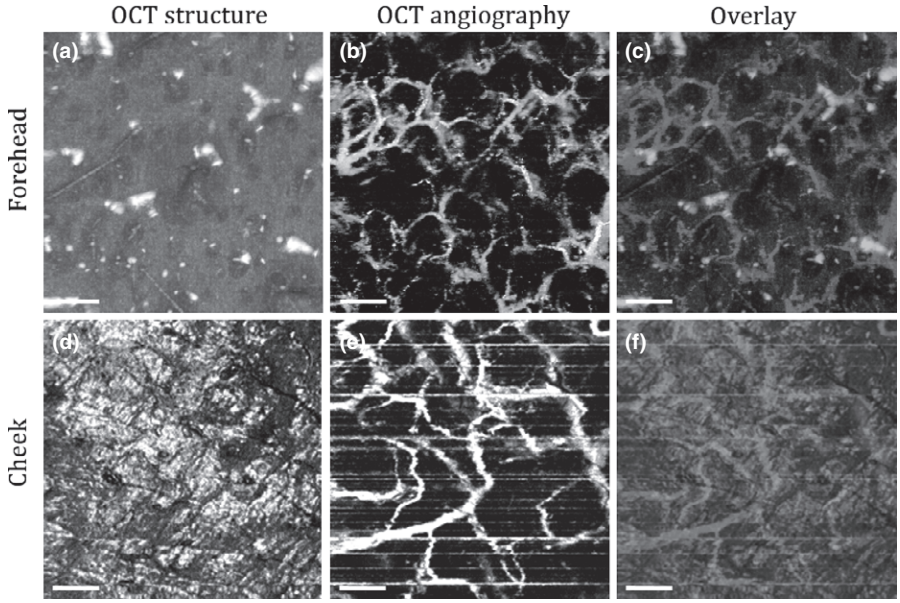

Fig. 3. In vivo optical coherence tomography (OCT) imaging of healthy facial skin tissues. Top panel: (a) En face structure image (3 mm ×3 mm) of forehead, (b) Its corresponding vasculature image, (c) Overlay of (a) with (b). Bottom panel: (d) En face structure image (3 mm × 3 mm) of cheek, (e) its corresponding vasculature image, (f) overlay of (d) with (e). Scale bars represent 0.5 mm.

diameter and less dense in Fig 3e. Multiple horizontal lines on the cheek angiogram (Fig. 3e) are image artifacts, which were caused by either involuntary head motion of the subject or hand shaking of the observer or both of them during imaging. Field of view of all images is 3 mm × 3 mm.

Structural and microvascular imaging on abnormal skin

There has been growing evidences suggesting that microvasculature plays a predominant role in pathogenesis of skin conditions such as acne, psoriasis, and skin cancer (29). To improve our understanding of the involvement of vascular abnormality in skin conditions, visualization and identification of vessels with a characteristic morphology are essential to assess many types of skin lesions. Hence, there is a need of non-invasive imaging tool to visualize the tissue microcirculation. In Section 3.1, we showed functional imaging ability of OCT on human skin tissues, allowing us to observe the vascular features of various normal skin tissue beds *in vivo*. In this section, the functional OCT imaging is expanded to the underlying skin conditions to explore vessel morphology in the cutaneous lesions.

Figure 4 shows OCT imaging results of three types of cutaneous conditions; acne, papules, and nevus, taken from different individual subjects. First to fourth columns of each panel in Fig. 4 represent a picture including the skin lesion, OCT structure image of the lesion (3 mm × 3 mm), corresponding OCT angiogram (3 mm × 3 mm), and their overlay. In the first panel, a picture shows acne at early stage, appearing small elevation of reddish skin. It has a pustule, containing a purulent material consisting of necrotic inflammatory cells. The OCT structure image is similar to the acne appearance in the picture. The OCT angiogram reveals a microvessel network in the acne region, consisting of dotted vessels corresponding to papillary dermal vessel and complex upper dermal plexus. Note that the OCT angiography signals were not observed at the pustule, implying no functional blood vessels innervating this region, probably due to that the fluid in pustule may be stagnant with limited Brownian motion of inflammatory cells.

Second and third panels in Fig. 4 show papules on arm and chest, appearing circumscribed, raised reddish spots on the skins with distinct borders as shown in pictures and OCT structure images. In their OCT angiograms, it is interesting to observe the vessel distribution patterns. The appearance of blood vessels in the papule on arm (second panel) is thick, irregular in shape with minimal branching. However, vessels in the papule on the chest

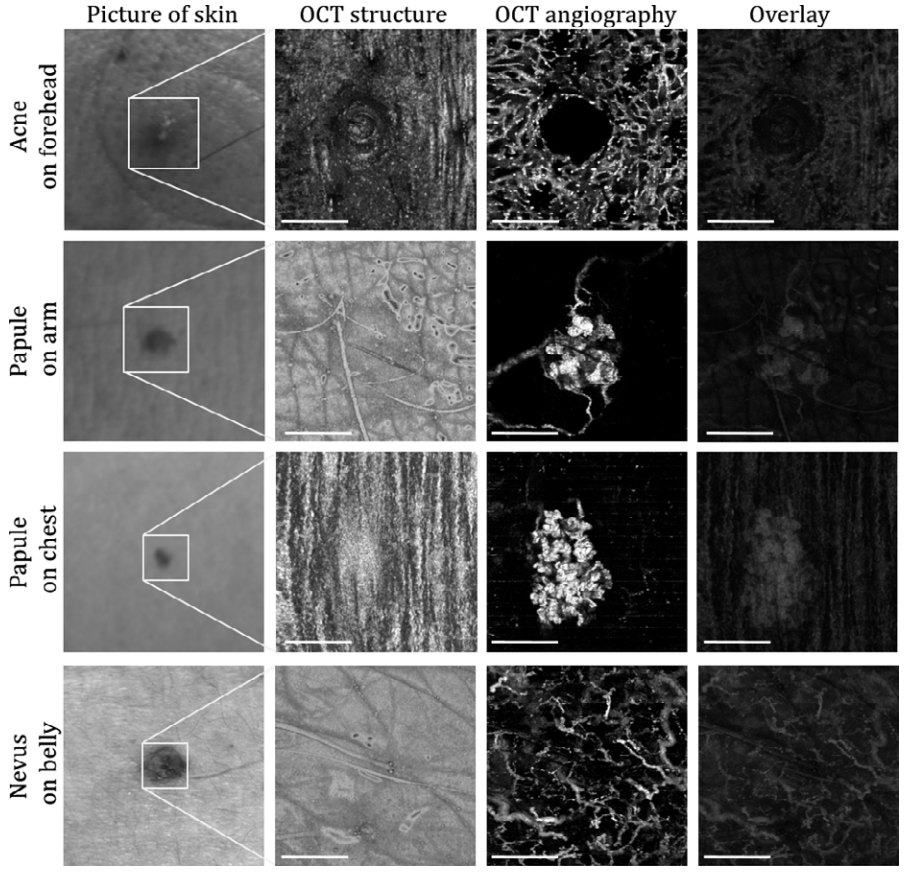

Fig. 4. In vivo optical coherence tomography (OCT) imaging of different skin lesions on human body. Top panel: acne on forehead. Second panel: red papule on arm. Third panel: red papule on chest. Bottom panel: nevus on belly. First to fourth columns for each panel are photograph of the skin lesion, OCT structure image, corresponding blood flow image, and their overlay, respectively. Size of all images (except for pictures) is 3 mm × 3 mm and scale bars represent 1.0 mm.

(third panel) look curled up and clustered through the lesion, resembling the glomerular apparatus.

Furthermore, nevus was examined on a subject's belly and its OCT results are described at bottom panel in Fig. 4. Nevus is an unusual benign mole with distinct boundary that may resemble melanoma (30). In the OCT angiogram, the vascular pattern of nevus was identified having irregular linear vessels that barely branch, which gives a favorable agreement to a result by classical dermascopy (31).

Structural and microvasculature imaging on a wounded skin

Disruption of cutaneous epidermal–dermal continuity is defined as a wound. Following the occurrence of a wound, skin integrity is rapidly restored through multiple interrelated overlapping biological phases known as inflammation, cellular proliferation, and maturation. During the healing process, characteristics of structural and microvascular changes in the tissue are unique to each stage of healing.

The OCT images of a wounded human skin during healing stages are shown with great detail in Fig. 5, thanks to the large field of view (5 mm × 5 mm). Here, cross-sectional OCT images in Fig. 5a–c show the structural remodeling in the epidermis and D. OCT en face structural (Fig. 5d and e) and microvascular images (Fig. 5g–i) are used to better visualize and locate the wound lesion borders. In the early stages of wound healing microvasculature is sparsely organized in wound region than those in the surrounding normal tissue as shown in Fig. 5g and h, however, it becomes progressively denser in the maturation stage. Structural images are merged with the microvasculature and shown in Fig. 5j–l.

Discussion

Emerging digital imaging methods take place of classical 'cold light' examination by providing

the superior ability of visualizing, monitoring, quantitating, and classifying morphologic changes during various cutaneous processes. However, most of these methods are used only in characterizing structural changes in tissue beds and are difficult to provide blood perfusion maps at a capillary level. OCT-based microangiography provides additional information about the extent of injury by providing a high-resolution map of functional microvasculature. This is exemplified in Figs 4 and 5, where utilizing OMAG features along with OCT structural images promises a better strategy for assessing the condition of abnormal skin condition than just relying on structural images.

Cutaneous wound is usually created as a result of damage to the skin after an injury, and its healing process consists of overlapping multiphase processes including hemostasis, inflammation, tissue formation, and tissue remodeling. Understanding this complicated healing process and developing strategies for better wound healing outcomes have been active fields of research (32). Various growth factors such as vascular endothelial growth factor, transforming growth factor-beta and fibroblast growth factor are currently attracting clinical interests to promote the healing process (33). As shown in Fig. 5, OCT microangiography could provide direct visualization and quantitation of the *in vivo* microvascular changes during wound healing and may be utilized in the studies involving these growth factors. Similarly, it may also be applied to other studies with topical drugs and stem cell therapies, in which OMAG can serve as a real-time monitor tool to provide feedbacks to the treatment strategy about the therapeutic effects on wound healing, thus improving the treatment outcomes.

Furthermore, cutaneous microcirculation is usually first to malfunction in several diseases such as primary Raynaud's phenomenon (34), systemic sclerosis (35), port wine stain (36), psoriasis (14), and skin cancer (37). With OMAG, vessel density of various parts of the normal and abnormal skins can easily be calculated (38), and used as a prognostic or diagnostic marker to assess progression and regression of the skin lesions, replacing a standard visual inspections. Various non-invasive microvascular reactivity tests have been utilized in clinics i.e. mechanical/thermal/electrical stimuli (39–41) or subdermal injections of pharmacological agents (39). However, due to the limitations of the current available blood perfusion imaging techniques such as laser Doppler imaging (42)

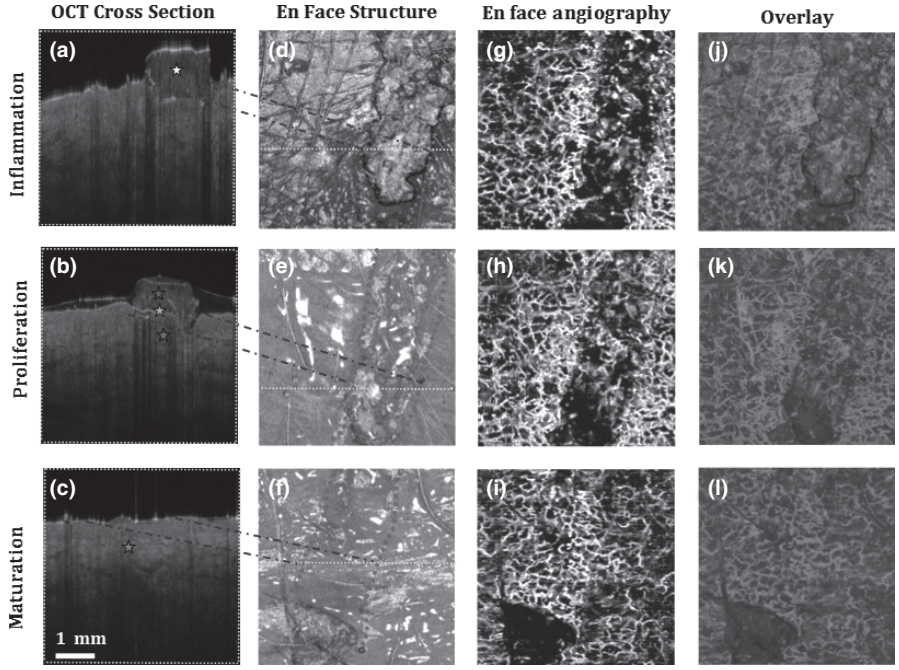

Fig. 5. Images from the inflammation, proliferation, and maturation stages of wound healing over 10 days. (a–c) Optical coherence tomography (OCT) cross-sectional views of the areas marked with yellow-dashed lines in en face images (d–f). In (a), yellow dot points to inflammatory edema formation. In (b), blue, green and red dots point to hemostatic crust, re-epithelialization, and dermal regeneration, respectively. In (c), purple dot points to healed dermal layer. (d–f) maximum intensity projection (MIP) of OCT en face structural images. (g–i) Optical microangiography (OMAG) MIP of microvasculature at 0–1 mm depth. Red dotted lines show the wound area. (j–l) Overlay of (d–f) with (g–i).

and laser speckle contrast imaging (43), they are often used to provide gloss assessment of skin blood perfusion. OCT microangiography would make these tests possible to be assessed more accurately and objectively with its unprecedented capability of visualizing detailed microvascular network innervating skin tissue, at a level of capillary vessels.

Optical coherence tomography has been a revolutionary tool in clinical ophthalmology, but it has not been widely adopted in clinical dermatology yet. The reasons may be summarized as the difficulty of articulating functional properties of OCT on human subjects and its relatively high cost compared to simple and well-established techniques used in dermatology. Recent developments of high-speed reliable swept laser sources and novel OCT angiography methods such as OMAG would make the OCT system more user friendly with lower cost, attractive to clinicians.

Although OCT technology has made great progress over the last decade, there are still some caveats. First, motion induced noise can deteriorate the angiography quality significantly, as can be seen in Fig. 2e. The use of a vacuum cushion is a simple, commonly used method to limit the motion at the hand and forearm (41), but motion tracking systems (44) should be employed for clinical dermatology applications on other parts. Moreover, the limited penetration depth of OCT prevents its applications from imaging the desired location that is more than 2 mm in depth. Luckily, the development of endoscopic probes (45) using MEMS scanners (46) are surging and it can extend the use of OCT in clinics.

Conclusion

Based on the presented results, OCT-based microangiography promises significant advantages compared to alternative imaging methods used in clinical dermatology by utilizing OMAG. Here, we have shown the use of OCT on different parts of human body, with or without abnormality, and demonstrated the capabilities of OMAG for better visualization of cutaneous wound healing process on human. Future well-designed clinical studies will be required to systematically investigate and establish the benefits of this technology, contributing to the clinical management and improvement of new treatment alternatives.

Acknowledgements

The study was supported in part by National Institutes of Health grants (R01HL093140 and R01EB009682).

References

1. Abramovits W, Stevenson LC. Changing paradigms in dermatology: new ways to examine the skin using noninvasive imaging methods. Clin Dermatol 2003; 21: 353–358.
2. Kittler H, Pehamberger H, Wolff K, Binder M. Diagnostic accuracy of dermoscopy. Lancet Oncol 2002; 3: 159–165.
3. González S, Swindells K, Rajadhyaksha M, Torres A. Changing paradigms in dermatology: confocal microscopy in clinical and surgical dermatology. Clin Dermatol 2003; 21: 359–369.
4. Kumagai K, Koike H, Nagaoka R, Sakai S, Kobayashi K, Saijo Y. High-resolution ultrasound imaging of human skin in vivo by using three-dimensional ultrasound microscopy. Ultrasound Med Biol 2012; 38: 1833–1838.
5. Tomlins PH, Wang RK. Theory, developments and applications of optical coherence tomography. J Phys D Appl Phys 2005; 38: 2519.
6. Cobb MJ, Underwood RA, Li X, Usui ML, Chen Y, Olerud J. Noninvasive assessment of cutaneous wound healing using ultrahigh-resolution optical coherence tomography. J Biomed Optics 2006; 11: 064002–064002.
7. Gambichler T, Orlikov A, Vasa R, Moussa G, Hoffmann K, Stücker M, Bechara FG. In vivo optical coherence tomography of basal cell carcinoma. J Dermatol Sci 2007; 45: 167–173.
8. Mogensen M, Nürnberg BM, Forman JL, Thomsen JB, Thrane L, Jemec GBE. In vivo thickness measurement of basal cell carcinoma and actinic keratosis with optical coherence tomography and 20-MHz ultrasound. Br J Dermatol 2009; 160: 1026–1033.
9. Yano K, Kajiya K, Ishiwata M, Hong YK, Miyakawa T, Detmar M. Ultraviolet B-induced skin angiogenesis is associated with a switch in the balance of vascular endothelial growth factor and thrombospondin-1 expression. J Investig Dermatol 2004; 122: 201–208.
10. Baran U, Li Y, Wang RK. In vivo tissue injury mapping using OCT based methods. Appl Opt 2015; 54: 6448–6453.
11. Greaves NS, Benatar B, Whiteside S, Alonso-Rasgado T, Baguneid M, Bayat A. Optical coherence tomography: a reliable alternative to invasive histological assessment of acute wound healing in human skin? Br J Dermatol 2014; 170: 840–850.
12. Wang RK, Jacques SL, Ma Z, Hurst S, Hanson SR, Gruber A. Three dimensional optical angiography. Opt Express 2007; 15: 4083–4097.
13. Yousefi S, Zhi Z, Wang RK. Label-free optical imaging of lymphatic vessels within tissue beds in vivo. IEEE J Sel Top Quantum Electron 2014; 20: 15–24.
14. Qin J, Jiang J, An L, Gareau D, Wang RK. In vivo volumetric

imaging of microcirculation within human skin under psoriatic conditions using optical microangiography. Lasers Surg Med 2011; 43: 122–129.
15. Li Y, Baran U, Wang RK. Application of thinned-skull cranial window to mouse cerebral blood flow imaging using optical microangiography. PLoS ONE 2014; 9: e113658.
16. Baran U, Li Y, Wang RK. Vasodynamics of pial and penetrating arterioles in relation to arteriolo-arteriolar anastomosis after focal stroke. Neurophotonics 2015; 2: 025006–025006.
17. Baran U, Shi L, Wang RK. Capillary blood flow imaging within human finger cuticle using optical microangiography. J Biophotonics 2015; 8: 46–51.
18. Choi WJ, Wang RK. In vivo imaging of functional microvasculature within tissue beds of oral and nasal cavities by swept-source optical coherence tomography with a forward/side-viewing probe. Biomed Opt Express 2014; 5: 2620–2634.
19. Wang H, Baran U, Wang RK. In vivo blood flow imaging of inflammatory human skin induced by tape stripping using optical microangiography. J Biophotonics 2015; 8: 265–272.
20. Yousefi S, Qin J, Dziennis S, Wang RK. Assessment of microcirculation dynamics during cutaneous wound healing phases in vivo using optical microangiography. J Biomed Optics 2014; 19: 076015–076015.
21. Baran U, Li Y, Choi WJ, Kalkan G, Wang RK. High resolution imaging of acne lesion development and scarring in human facial skin using OCT-based microangiography. Lasers Surg Med 2015; 47: 231–238.
22. Laser Institute of America. American national standard for safe use of lasers ANSI Z136.1-2000. New York, NY: American National Standards Institute Inc., 2000.
23. Choi WJ, Reif R, Yousefi S, Wang RK. Improved microcirculation imaging of human skin in vivo using optical microangiography with a correlation mapping mask. J Biomed Optics 2014; 19: 036010–036010.
24. Enfield J, Jonathan E, Leahy M. In vivo imaging of the microcirculation of the volar forearm using correlation mapping optical coherence tomography (cmOCT). Biomed Opt Express 2011; 2: 1184–1193.
25. An L, Qin J, Wang RK. Ultrahigh sensitive optical microangiography for in vivo imaging of microcirculations within human skin tissue beds. Opt Express 2010; 18: 8220–8228.
26. Wang RK, An L, Francis P, Wilson DJ. Depth-resolved imaging of capillary networks in retina and choroid using ultrahigh sensitive optical microangiography. Opt Lett 2010; 35: 1467–1469.
27. Cutolo M, Grassi W, Matucci Cerinic M. Raynaud's phenomenon and the role of capillaroscopy. Arthritis Rheum 2003; 48: 3023–3030.
28. Smith V, Riccieri V, Pizzorni C, Decuman S, Deschepper E, Bonroy C, Sulli A, Piette Y, De Keyser F, Cutolo M. Nailfold capillaroscopy for prediction of novel future severe organ involvement in systemic sclerosis. J Rheumatol 2013; 40: 2023–2028.
29. Braverman IM. The cutaneous microcirculation. J Investig Dermatol Symp Proc 2000; 5: 3–9. Nature Publishing Group.
30. Arumi-Uria M, McNutt NS, Finnerty B. Grading of atypia in nevi: correlation with melanoma risk. Mod Pathol 2003; 16: 764–771.
31. Martín JM, Rubio M, Bella R, Jordá E, Monteagudo C. Complete regression of melanocytic nevi: correlation between clinical, dermoscopic, and histopathologic findings in 13 patients. Actas Dermosifiliogr (English Edition) 2012; 103: 401–410.
32. Menke NB, Ward KR, Witten TM, Bonchev DG, Diegelmann RF. Impaired wound healing. Clin Dermatol 2007; 25: 19–25.
33. Frank S, Hübner G, Breier G, Longaker MT, Greenhalgh DG, Werner S. Regulation of vascular endothelial growth factor expression in cultured keratinocytes. Implications for normal and impaired wound healing. J Biol Chem 1995; 270: 12607–12613.
34. Tooke JE. Microvascular function in human diabetes: a physiological perspective. Diabetes 1995; 44: 721–726.
35. Sulli A, Secchi ME, Pizzorni C, Cutolo M. Scoring the nailfold microvascular changes during the capillaroscopic analysis in systemic sclerosis patients. Ann Rheum Dis 2008; 67: 885–887.
36. Liu G, Jia W, Nelson JS, Chen Z. In vivo, high-resolution, three-dimensional imaging of port wine stain microvasculature in human skin. Lasers Surg Med 2013; 45: 628–632.
37. Johnson KE, Wilgus TA. Multiple roles for VEGF in non-melanoma skin cancer: angiogenesis and beyond. J Skin Cancer 2012; 2012: 483439.
38. Reif R, Qin J, An L, Zhi Z, Dziennis S, Wang R. Quantifying optical microangiography images obtained from a spectral domain optical coherence tomography system. J Biomed Imaging 2012; 2012: 9.
39. Cracowski JL, Minson CT, Salvat-Melis M, Halliwill JR. Methodological issues in the assessment of skin microvascular endothelial function in humans. Trends Pharmacol Sci 2006; 27: 503–508.
40. Minson CT. Thermal provocation to evaluate microvascular reactivity in human skin. J Appl Physiol 2010; 109: 1239–1246.
41. Roustit M, Cracowski JL. Non-invasive assessment of skin microvascular function in humans: an insight into methods. Microcirculation 2012; 19: 47–64.
42. Clark S, Campbell F, Moore T, Jayson M IV, King TA, Herrick AL. Laser Doppler imaging—a new technique for quantifying microcirculatory flow in patients with primary Raynaud's phenomenon and systemic sclerosis. Microvasc Res 1999; 57: 284–291.
43. Roustit M, Millet C, Blaise S, Dufournet B, Cracowski JL. Excellent reproducibility 1 of laser speckle contrast imaging to assess skin microvascular reactivity. Microvasc Res 2010; 80: 505–511.
44. Zhang QQ, Huang Y, Zhang T, Kubach S, An L, Laron M, Sharma U, Wang RK. Wide-field imaging of retinal vasculature using optical coherence tomography-based microangiography provided by motion tracking. J Biomed Opt 2015; 20: 066008.
45. Qiu Z, Piyawattanametha W. MEMS-based medical endomicroscopes. IEEE J Sel Top Quantum Electron 2015; 21: 1–16.
46. Holmstrom ST, Baran U, Urey H. MEMS laser scanners: a review. J Microelectromech Systems 2014; 23: 259–275.

Address:
R. K. Wang
Department of Bioengineering
University of Washington
3720 15th Ave NE
Seattle, WA 98195, USA
Tel: +1 206 6165025
Fax: +1 206 6853300
e-mail: wangrk@uw.edu